

## Feedback Control of Resistive Wall Modes in Reversed Field Pinches.

R. Paccagnella<sup>1</sup>, D. Gregoratto<sup>2</sup>, A. Bondeson<sup>2</sup>, Y.Q.Liu<sup>2</sup>

<sup>1</sup>*Consorzio RFX, Associazione EURATOM-ENEA sulla fusione, Padova, Italy  
and Consiglio Nazionale delle Ricerche, Roma, Italy*

<sup>2</sup>*Department of Electromagnetics, EURATOM-VR/Fusion Association Chalmers  
University of Technology, S-412 96 Göteborg, Sweden*

**1. Introduction** For reversed field pinches (RFP's) the control of MHD modes is a very important issue. In RFX, encouraging results have been obtained by applying an external  $m = 0$  perturbation to induce rotation of the locked modes[1]. Here we analyze the problem of linear feedback stabilisation of the nonresonant modes in a RFP, in the presence of a resistive wall surrounding the plasma.

We generalize the calculations of Fitzpatrick and Yu [2], to include discrete coil effects in the poloidal direction and treat a system of  $M_c$  (poloidal)  $\times$   $N_c$  (toroidal) coils and sensors pairs. The stability and robustness is analyzed for different geometries of the system (number and dimension of coils), and for different feedback signals (sensor measurements of radial, poloidal and toroidal magnetic field perturbation).

We will first use a simple proportional current control scheme, in which the applied current in the coils is proportional to the perturbation measured at the sensors. The analysis of the stability of the feedback scheme is based on the Nyquist stability criterion and requires knowledge of the transfer function between the current in the coils and the magnetic field at the sensor to be known. In many cases the stabilisation is possible with proportional gain  $K_p$  only in some window  $K_{p,min} \leq K_p \leq K_{p,max}$ . The lower and upper limits depend on the geometry and on the type of sensor. Preliminary results from the more realistic model of voltage control are also reported.

**2. Plasma and feedback system.** We consider a cylindrical plasma of radius  $a$  with periodicity  $2\pi R$  along the axis and aspect ratio  $R/a = 4$ . The plasma is surrounded by a resistive wall with radius  $r_w = 1.1a$  and  $\tau_w = 50$ ms is the decay time for an  $m = 1$  shell mode. The mode spectrum has been determined for an ideal plasma with zero pressure and for two different equilibria, respectively low- $\Theta$  ( $F = -0.2$ ,  $\Theta = 1.58$ ) and high  $\Theta$  ( $F = -0.88$ ,  $\Theta = 2.07$ ). The study only regards the stabilisation of the unstable  $m = 1$  nonresonant modes,  $-6 \leq n \leq +3$  and  $n = -7, +1 \leq n \leq +4$  respectively.

A set of  $M_c \times N_c$  equidistant feedback coils is placed at  $r_f = 1.25a$ . The coils are modeled as thin wires and a design parameter that has been considered is the coil angular dimension  $\Delta\theta \times \Delta\phi$ . The sensors are located with similar angular distribution on the resistive wall, centered on the geometrical axis of the coil, and can measure the perturbed radial, poloidal or toroidal fields. Radial small sensors measure the radial local field while radial wide sensors measure the average field on the angle subtended by the companion coil. For the poloidal and toroidal sensors, we have considered measurements both on the internal or external side of the wall.

**3. Current control.** We analyze the independent control of each of the Fourier components in the perturbation as superposition of signals from the different sensors. To determine the transfer function for the magnetic field measured at the sensor  $b_s$ , due to the current in the feedback coil  $I_f$ , we will use the same procedure as in [3, 4].

The electromagnetic model involves the  $\Delta'$  values at the resistive wall (for a plasma in absence of feedback) and standard matching conditions at the resistive wall  $r = r_w$  and feedback coil radius  $r = r_f$ .

For each Fourier component the magnetic field at the sensor  $b_{mn}^s$  can be related to the currents in the coil by introducing the surface current density  $\nabla J_f \times \hat{r}$ :

$$b_{mn}^s = M_{mn}^s b_{mn}^f = M_{mn}^s c_{mn} J_{mn}^f$$

where  $b_{mn}^f$  is the magnetic field at the coils surface  $r = r_f$ , produced by only the currents in the coil. We observe that the finite number of sensors and coils give rise to so called sideband effects [2, 4]. The Fourier decomposition of the measured signal can not decouple the information of modes with mode numbers separated by multiples of the number of coils  $M_c$  and  $N_c$ . Similarly, each single current harmonic in the coils generates an infinite number of harmonics with mode numbers separated by multiples of the number of coils. The final transfer function for the  $(m, n)$  Fourier component, normalized to be adimensional is

$$P_{1,mn} = \frac{\pi a}{\mu_0} \frac{b_{mn}}{I_{mn}^f} = \sum_{m'=m+lM_c} \sum_{n'=n+pN_c} S_{m'n'} M_{m'n'}^s c_{m'n'} F_{m'n'}$$

where  $S$  and  $F$  are shape factors for the sensors and the coils and the summation includes all the sidebands of the mode  $(m, n)$ . In the following we will neglect the indexes  $(m, n)$  in the notation. The characteristic equation for the system is  $1 + K(s)P_1(s) = 0$ , where  $K(s)$  is the gain of the controller. The system is stable if all the roots of the characteristic equation lie in the negative half-plane. The Nyquist stability criterion implies that when there is one unstable RWM for the chosen  $(m, n)$ , the system is stable if the plot of the transfer function  $P_1(j\omega)$  with  $-\infty < \omega < \infty$  encircles counterclockwise the point  $(-1, 0)$  in the complex plane. In general this will happen only for a limited range of values for the gain.

To avoid more than one unstable pole in  $P_1(s)$ , the control system must not couple two unstable modes through the sideband effect. This imposes a lower limit in the number of coils. For the two equilibria we have examined with rather different  $\Theta$ , it is necessary to have  $M_c > 3$  and  $N_c > 11$  to avoid the coupling of two nonresonant mode. We also require that the system should not couple the mode we are trying to stabilise to any of the (resistive) internally resonant modes, the *dynamo* modes. This is achieved if  $M_c = 4$  and  $N_c = 24$ .

Overlapping the coils can slightly decrease the required gain for the stabilisation but it is not considered a practical solution. The best solution in terms of minimum gain is therefore with coils covering completely the wall surface without overlapping. All the types of sensor can in principle be used if the gain is chosen appropriately. Fig.1 shows Nyquist plots of  $P_1(i\omega)$  with  $0 < \omega < \infty$  for all the different types of sensors and the most unstable mode,  $m = 1, n = -6$ . For this case the stabilisation with a radial wide sensor (rw) requires the highest gain. Particular care must be taken in choosing the gain

for the external poloidal and toroidal sensors (p+ and t+). The gain is limited both from below and above. In the following we will not consider these sensors.

We have studied the critical gain as function of the toroidal width of the coil  $\Delta\phi_f$ , when the poloidal amplitude of the coils has been fixed,  $\Delta\theta_f = 90^\circ$ . We find that for small radial and toroidal sensors, the gain is limited also from above for some modes.

Fig.2 shows the limiting curves for the critical gain as function of  $\Delta\phi_f$  for both equilibria. The lower and upper limit curves are built by considering the most stringent condition imposed by all the unstable modes. The lower limit for the gain is generally set by the most unstable mode. For non overlapping coils ( $\Delta\phi \leq 15^\circ$ ) the poloidal and toroidal sensors can operate within a larger range of values for the coil width than the radial sensors. Furthermore, poloidal sensors have the advantage of not presenting an upper limit  $K_{max}$  to the gain for any of the coil widths. But in practice the toroidal sensors are preferred due to the more favourable signal/noise ratio in an RFP. In general there exists a window in coil width where each of the sensors can stabilise all the modes if the gain is chosen appropriately.

**5. Voltage control.** We have also considered a more realistic control system, in which the voltage measured at the sensor is fed back to the system and controls the voltage applied to the coil,  $V_f(s) = -K(s)V_s$ . The controller  $K$  can also have a derivative and an integral action:

$$K(s) = \left( K_p + \frac{K_i}{s} \right) W(s), \quad W(s) = \frac{sT_d + 1}{sT_d/\xi + 1}$$

The parameters in the controller have been optimized in order to stabilise the system with the lowest applied voltage and by satisfying requirements on the stability and robustness of the control.

We combine the electromagnetic models in [3, 4] to determine the loaded self inductance  $L_f^{loaded}$  of the feedback coils taking into account currents induced in the plasma-wall system. The standard self-inductance  $L_f^0$  is known from measurements.

The transfer function  $P_2(s)$  can be introduced by defining the total flux linked to the active coil as

$$\psi_f(s) = L_f^{loaded} I = (L_f^0 + L_f^{ext}) I = P_2(s) L_f^0 I$$

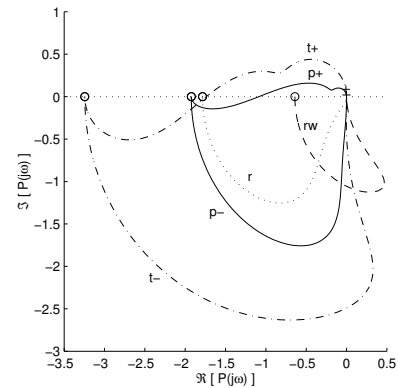


Figure 1: Nyquist plots of open loop transfer function for radial sensors, small (dotted) and wide (dashed), internal and external poloidal (solid) and toroidal (dash-dotted) sensors.

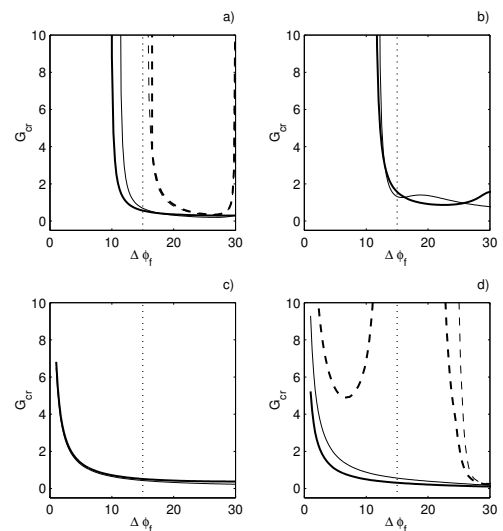


Figure 2: Minimum (solid line) and maximum (dashed line) gain  $K_{cr}$  necessary to stabilise all the modes, as function of the toroidal width of the coils, for (a) radial small, (b) radial wide, (c) poloidal internal, (d) toroidal internal sensors. Bold lines refer to the equilibrium  $\Theta = 1.58$  and normal lines to  $\Theta = 2.07$ .

where  $I$  is the current in the coil. If the distance between the feedback coils and the wall is increased then  $P_2 \rightarrow 1$ .

The total transfer function will finally be determined by considering the voltage across the feedback coil

$$V_f(s) = s\psi_f(s) + R_f I = -K(s)V_s(s) \quad (1)$$

where  $R_f$  is the coil resistance and the voltage at the sensor is  $V_s(s) = s\psi_s(s) = sP_1(s)L_f^0 I$ . With  $\tau_f = L_f^0/R_f$  the characteristic time of the coil, the total voltage-to-voltage transfer function becomes

$$P(s) = \frac{\tau_f s P_1(s)}{1 + \tau_f s P_2(s)}$$

and the characteristic equation of the closed loop system is  $1 + K(s)P(s) = 0$ . As in [3] we assume that the controller is switched on when the sensor signal exceeds a chosen threshold

value  $b_0$  and a reasonable value in RFX would be about 0.3mT.

In RFX,  $\tau_f/\tau_w \approx 0.1$  implies that the voltage is mainly resistive in the active coil. This makes it possible to use a simple integral controller,  $K_i \neq 0$ ,  $K_p = 0$  and  $W = 0$ . Note that in this situation, the role of  $K_i$  and  $K_p$  could be exchanged if instead of the sensor voltage we had used a magnetic field measurement. Fig.3 shows the time evolution of feedback voltage, current and magnetic perturbation for the poloidal sensor case. The mode considered here is the most unstable ( $m = 1, n = -6$ ) for the low- $\Theta$  equilibrium. The peak value of the voltage,  $V_{max} \approx 10V$ , can be reduced if the requirement on the settling time (the duration of the transient) is less stringent. The minimum peak voltage for this case is about 5 Volts (with twice the settling time) and is limited by a constraint on the stability of the controller. We have adopted a standard control criterion that should guarantee sufficient stability. The shortest distance from the loop  $K(j\omega)P(j\omega)$  to the instability point  $(-1,0)$  is here lower bounded by 0.5.

The controller optimization is in progress for all the different sensors. More complex controller could for instance enlarge the operational window in  $\Delta\phi_f$  for toroidal sensors. Further work will be made to apply the theory to the RFX control system.

## References

- [1] Bartiromo R., Bolzonella T., Buffa A., Chitarin G., Martini S., Masiello A., Ortolani S., Piovan R., Sonato P., and Zollino G, Phys. Rev.Lett **83**, 1779 (1999)
- [2] R. Fitzpatrick and E. P. Yu, Phys. Plasmas **6** 3536 (1999) .
- [3] A. Bondeson, Yueqiang Liu, D. Gregoratto, Y. Gribov and V.D. Pustovitov, Nucl. Fusion **42**, 768-779 (2002)
- [4] R. Paccagnella, D. Gregoratto, A. Bondeson, accepted for publication on Nucl. Fusion.

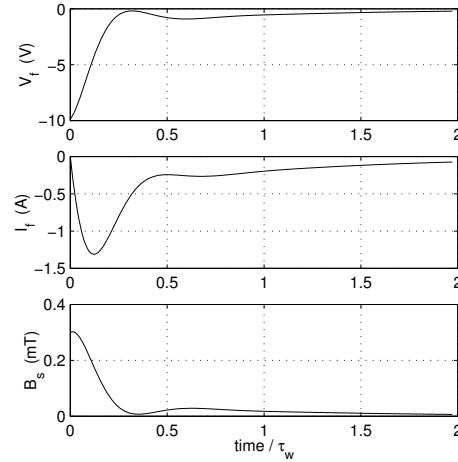


Figure 3: Time evolution of the feedback voltage  $V_f$ , current  $I_f$  in the coil and magnetic field perturbation  $B_s$  at the sensors. The time is normalised to the wall time.